Larhyss Journal, ISSN 1112-3680, n°60, Dec 2024, pp. 87-111

DYNAMIC WATERSHED MODELLING: HEC-HMS ANALYSIS OF A TROPICAL WATERSHED

KHERDE R.V. [1*]***, MEHTA D.J.***[2]***, MORE K.C.*** [3]***, SAWANT P.H.***[4]

[1, 3] D.Y. Patil University Ambi Pune, Maharashtra, India
[2] Government College of Engineering, Surat, Gujrat, India
[4] Sardar Patel College of Engineering, Mumbai, Maharashtra, India

(*) rkherde@gmail.com

Research Article – Available at http://larhyss.net/ojs/index.php/larhyss/index
Received April 2, 2024, Received in revised form November 22, 2024, Accepted November 24, 2024

ABSTRACT

The advancement of computational hydraulic simulations has reached an impressive zenith, markedly enhancing our comprehension of anthropogenic influences on fluvial dynamics and the intricacies of sustainable hydrological stewardship. The extensively utilized HEC-HMS model, a creation of the US Army Corps of Engineers, remains deficient in tailored calibration for Indian catchments. This scholarly inquiry sought to evaluate the applicability of HEC-HMS version 4.10 to the designated study area, employing three distinct calibration methodologies: the deficit and constant loss approach, the Soil Conservation Service Curve Number (SCS-CN) method, and the Green and Ampt infiltration model. The principal objective was to ascertain the optimal simulation technique aligning with the unique characteristics of the study catchment. A meticulous investigation within the Wardha River catchment encompassed an 18-year dataset, comprising daily precipitation and temperature records procured from the Indian Meteorological Department (IMD), captured at a refined spatial granularity of 0.25° × 0.25°. Additionally, daily potential evapotranspiration, computed via the Hargreaves Equation, was integrated. The dataset was further augmented by daily discharge data from the India Water Resources Information System, specifically from the Sirpur gauge station outlet, spanning the years 2001 to 2018, facilitating a profound hydrological analysis. GIS layers were integrated into the calibration process using HEC-HMS 4.10, enhancing the hydrological modeling and analysis. After the calibration phase (2001-2010), the model was evaluated with new data from 2011-2018 using metrics like RMSE, NSE, and R^2. The empirical results indicated that the most reliable flow simulations were obtained through the integration of the Soil Conservation Service Curve Number (SCS-CN) loss method with the SCS unit hydrograph approach, outperforming the Clark unit hydrograph and Snyder unit hydrograph methods. However, it is imperative to note that the utilization of the SCS-CN method as the loss mechanism did not yield satisfactory outcomes when combined with the Snyder unit hydrograph method. Conversely, the Deficit and Constant

Loss method and the Green and Ampt infiltration model showed similar performance metrics, including NSE, with all three unit hydrograph methods. This uniformity underscores their robustness and reliability in generating consistent hydrological simulations within the specific context of the study.

Keywords: HEC-HMS, Rainfall runoff Modelling, Clark unit Hydrograph, Snyder unit Hydrograph, SCS-CN Unit Hydrograph

INTRODUCTION

Hydrological simulation modeling, an indispensable instrument within the realm of hydrology and water resources management, involves the utilization of intricate mathematical and computational models to replicate the multifaceted dynamics of the hydrological cycle (Kamagate et al., 2017; Herrera et al. 2022). This cycle includes processes like rainfall patterns, surface runoff, infiltration, evaporation, and groundwater flow (Chibane and Ali-Rahmani, 2015; Koua et al., 2019; Atallah et al., 2024). These sophisticated models serve as invaluable tools for researchers, engineers, and policymakers, facilitating their comprehension and prognostication of the intricate movement of water through diverse hydrological domains such as watersheds, river basins, and other complex water systems (Kouamé et al., 2017; Hariri Asli and Hozouri, 2021; Kupzig et al. 2023).

These models are pivotal in the forecasting and mitigation of flood occurrences by emulating how factors like rainfall and nival melt contribute to heightened fluvial discharge and potential flood events (Lin et al., 2022; Hafnaoui et al., 2023; Abd Rahman et al., 2023). Furthermore, hydrological models are indispensable for the efficacious management of water resources, encompassing activities like gauging water availability, designing reservoir structures, and optimizing the allocation of water resources (Liu et al., 2018; Bekhira et al., 2019; Rouissat and Smail, 2022). They also prove crucial when assessing the potential repercussions of land use modifications, the development of infrastructural projects, or the influence of climate change on the local hydrological system's dynamics (Remini, 2023; Nakou et al., 2023). Moreover, these models can serve as reliable prognosticators of drought conditions, engaging in the simulation of long-term pluviometric patterns and runoff behaviours (Hao et al., 2018; Benali Khodja and Ferdjouni, 2024).

It's imperative to underscore that the credibility and precision of hydrological models necessitate a comprehensive calibration process that aligns model parameters with historical data (Chibane and Ali-Rahmani, 2015; Fernando et al., 2021). In addition, validation exercises are essential to gauge the model's efficacy in predicting new, unobserved data points. Nonetheless, it's crucial to acknowledge that hydrological models grapple with uncertainties stemming from data quality and the inherent variability of model parameters (Kherde and Sawant, 2018). To address these uncertainties, rigorous uncertainty analyses are conducted to quantify and manage these inherent instabilities. Consequently, decision-makers are presented with a spectrum of potential outcomes, enhancing their capacity to make informed decisions (Rafiei et al., 2018). Verma et al.

(2024) examined uncertainty in hydrograph component estimation using the SUFI-2 algorithm with various objective functions, demonstrating how these functions influence calibration outcomes and parameter optimizations in hydrological models. Verma et al. (2023) simulated hydrological processes in the Mahanadi reservoir complex under different land use and climate change scenarios, revealing how these factors impact hydrological dynamics and water resources. Mehta et al. (2023) enhanced flood forecasting in the Narmada River Basin by combining hierarchical clustering with hydrological modeling, improving the accuracy and reliability of flood predictions. Kapadia et al. (2023) conducted flood hazard mapping in the lower Damanganga River Basin using a multi-criteria analysis and geoinformatics approach, providing valuable insights for flood risk management and mitigation strategies. In the paper of Hafnaoui et al. (2022), some of the local parameters that contribute to flooding in El Bayadh city in Algeria were analyzed. These include the constriction caused by urban expansion at the edges of Wadi Deffa, which crosses the city, considerably reducing its cross-section and thereby increasing the risk of flooding. Baudhanwala et al. (2023) evaluated the applicability of the SWMM model for urban flood forecasting in the western zone of Surat City, demonstrating its effectiveness in predicting flood events and managing urban flood risks.

Hydrological simulation modelling stands as an invaluable asset for comprehending and managing water resources, evaluating environmental repercussions, and making judicious choices concerning water-related issues, particularly in the face of the evolving landscape of climate change and escalating water scarcity challenges.

HEC-HMS, an abbreviation for the Hydrologic Engineering Centre's Hydrologic Modelling System, emerges as a preeminent computational tool devised under the aegis of the U.S. Army Corps of Engineers. This sophisticated software is paramount within the sphere of hydrological modelling, primarily orchestrating the simulation of the complex rainfall-runoff process inherent within watersheds and fluvial basins. HEC-HMS distinguishes itself as an all-encompassing and intricate modelling system, meticulously crafted to fulfil the requisites of engineers, hydrologists, and water resource specialists. It enables these professionals to engage in profound analytical and predictive endeavours concerning the metamorphosis of meteorological inputs, particularly precipitation, into resultant runoff and subsequent hydrological flow within a delineated watershed. This formidable instrument is predominantly harnessed to replicate the multifaceted process of transmuting rainfall into runoff, incorporating an array of intricate mechanisms such as infiltration, surface runoff, and the nuanced routing of hydrological flow through fluvial channels (Feldman, 2000). It avails itself to a versatile array of applications, accommodating an expansive range of watershed and river basin dimensions, from diminutive catchments to extensive and sprawling watersheds. Furthermore, HEC-HMS exhibits adaptability across diverse temporal resolutions, enabling users to operate within an extensive spectrum of temporal intervals, from the granular detail of hourly observations to the broader purview of daily aggregations (Hamdan et al., 2021). This temporal adaptability empowers users to effectively simulate and scrutinize a multitude of hydrological processes across varying temporal scales.

This software endows users with the capacity to input precipitation data, whether empirically observed or synthetically generated for simulation objectives. Within this paradigm, users are afforded the latitude to delineate intricate precipitation patterns and ascertain the return periods of these patterns, which are critical for design considerations and engineering evaluations (Yuan et al., 2019). HEC-HMS encompasses a rich repository of methodologies tailored to replicate hydrological losses encountered throughout the hydrological continuum. These losses encompass initial abstractions, the multifaceted process of infiltration, as well as evapotranspiration phenomena, all of which are pivotal in modulating the overarching hydrological dynamics (Sardoii et al., 2012). Additionally, the software extends its prowess through multifarious routing options for directing runoff through diverse conduits, reservoirs, and engineered constructs dispersed across the watershed. This multifaceted routing functionality enables the precise emulation of the complex pathways traversed by water within the hydrological system (Rad et al., 2022). Notably, HEC-HMS features an intuitive graphical interface that augments the processes of model creation and modification, facilitates data input, and furnishes a visual representation of simulation outputs. This user-centric interface is instrumental in enhancing the software's accessibility and fostering an efficient operational workflow. The scope of HEC-HMS's applications is vast, encompassing a myriad of scenarios, including but not limited to flood forecasting, flood risk assessment, storm water management strategies, reservoir operation optimization, and the design and analysis of hydraulic structures integral to diverse engineering projects (U.S. Army Corps of Engineers, 2008).

HEC-HMS incorporates a comprehensive assemblage of nine distinct loss methodologies, each serving specialized purposes, with some tailored for event-specific simulations and others engineered for continuous simulation scenarios (Halwatura and Najim, 2013). In the context of HEC-HMS, "loss methodologies" pertain to the mechanisms dictating how the model accounts for the reduction or depletion of precipitation within a watershed as it navigates various hydrological processes. These methodologies play a cardinal role in estimating the fraction of precipitation that is effectively converted into runoff. The precision in runoff estimation is indispensable for an array of hydrological and hydraulic analyses, including but not limited to flood forecasting and meticulous watershed management. The selection of a particular loss methodology is predicated on the inherent characteristics of the watershed under scrutiny and the availability of relevant data (Belay et al., 2022). Users thus engage in a thoughtful selection process, opting for the loss methodology that most aptly corresponds to the nuanced hydrological conditions of the specific geographic context.

Moreover, within HEC-HMS, a spectrum of seven distinct transformation methodologies is available to users. These "Transformation Methodologies" concern the intricate techniques employed to translate raw precipitation data into the dynamics of runoff or stream flow (Halwatura and Najim, 2013). These methodologies are an integral facet of the hydrological modelling enterprise, facilitating the precise emulation of the metamorphosis of precipitation, or other pertinent input variables, into actual hydrological flow within a watershed. The selection of a specific transformation methodology is contingent upon a plethora of considerations, including the watershed's

complexity, the availability and quality of relevant data, and the specific objectives of the hydrological modelling initiative (Belay et al., 2022). Users, in this decision-making process, conscientiously select the transformation methodology, or a combination thereof, that best aligns with the intricate hydrological processes of the watershed. This judicious selection ensures the model's capability to yield accurate and meaningful predictions regarding runoff dynamics.

METHODOLOGY

Study Area

The Wardha River Basin constitutes an extensive hydrological dominion nestled in the heart of India, predominantly straddling the states of Maharashtra with a minor extension into Madhya Pradesh. This basin encompasses the vast drainage network of the Wardha River alongside its interconnected tributaries, rendering it an essential component of the region's hydrological framework and ecosystem dynamics. Within this expansive hydrological landscape, the Wardha sub-basin delineates a geographic expanse defined by precise coordinates. This sub-basin unfurls within the geographic boundaries demarcated by latitudes 19°18’N to 21°58’N and longitudes 77°20’E to 79°45’E, encapsulating a strategically positioned and diverse region. The predominant fluvial artery within the basin is the Wardha River, which serves as a tributary on the right bank, eventually merging with the Pranhita River. This riverine system receives its sustenance from an intricate web of minor rivers and streams emanating from both the left and right banks. These contributing waterways bear appellations such as the Kar, Wena, Jam, Erai, Madu, Bembla, and Penganga, collectively sculpting the region's hydrological dynamics.

The catchment expanse of the Wardha River, a hydrological entity, encompasses an approximate area of 48,000 square kilometers, antecedent to the Sirpur gauge discharge station. This geographical sector wields considerable hydrological influence over the flow regimes of the Pranhita River, which in turn integrates into the larger fluvial framework of the Godavari River. Throughout its trajectory, the Wardha River navigates through heavily forested terrains, augmenting its ecological significance. The climatic conditions within the Wardha River Basin are tropical, characterized by an annual mean precipitation of approximately 1000 millimeters. This hyetographic input is crucial in maintaining the fluvial dynamics and the intricate ecosystems it supports, thereby underscoring its hydrological importance.

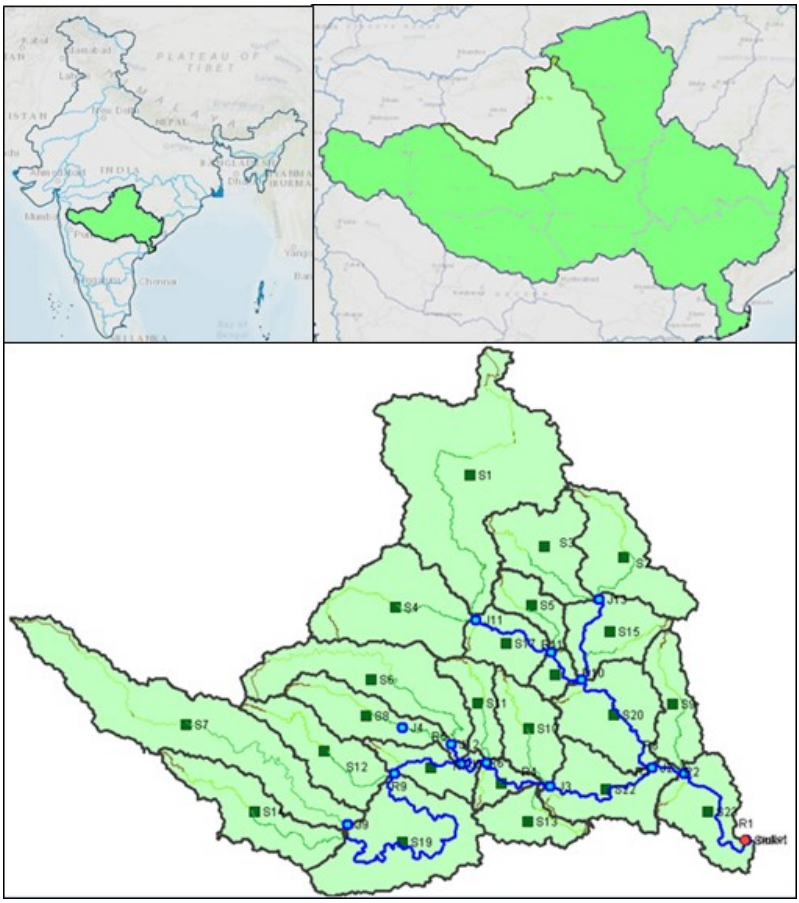

Figure 1: Location map of Wardha River Basin

The Wardha River Basin is distinguished by a complex mosaic of land use paradigms. It encapsulates a heterogeneous array of land types, including agrarian landscapes, lush forest biomes, urban agglomerations, and industrial sectors. The river is indispensable in facilitating agricultural productivity and providing essential hydric resources for the local populace, thereby serving as a linchpin for the regional economy. In essence, the Wardha River Basin stands as a pivotal geophysical and ecological region within central India. It is notable for its complex riverine network, diverse land use configurations, and its substantial contributions to agricultural activities and local economies. Moreover, it occupies a crucial role within the overarching structure of the Godavari River Basin system.

Data Collection

The investigatory endeavor undertaken within the fluvial expanse of the Wardha River catchment area was predicated upon an exhaustive compendium of data spanning an eighteen-year temporal continuum. This assemblage comprised quotidian gridded pluviometric data meticulously collated by the Indian Meteorological Department (IMD), with granularity manifesting at an exquisite spatial resolution of 0.25° × 0.25°, duly considering both latitudinal and longitudinal coordinates. Additionally, thermometric readings were procured from the IMD, and diurnal potential evapotranspiration metrics were deduced employing the Hargreaves Equation. The hydrological discharge records encompassing the period from 2001 to 2018 were sourced from the India Water Resources Information System (indiawris.gov.in/wris/#/RiverMonitoring), specifically for the Sirpur gauge discharge station situated at the fluvial terminus. To augment the calibration regimen of the Wardha catchment, Geographic Information System (GIS) stratifications were scrupulously developed and adroitly integrated into the analytical paradigm utilizing the HEC-HMS 4.10 software.

Data map preparation

We acquired high-resolution SRTM 1 Arc-Second Global (30m) digital elevation model tiles from the USGS portal, accessible at https://earthexplorer.usgs.gov/. These discrete tiles underwent a process of amalgamation to form a consolidated Digital Elevation Model (DEM) using the mosaicking feature within the QGIS software. Subsequently, the DEM dataset for the Wardha River basin was imported into HEC-HMS 4.1. Here, we utilized advanced Geographic Information System (GIS) tools to meticulously delineate the precise boundaries of the river basin. Figure 1 visually represents a sub-basin map of the Wardha River basin, detailing various sub-basins, their centroids, and the intricate stream network. Employing a specialized basin model, we conducted detailed calculations to determine key metrics such as individual sub-basin areas, total catchment area, longest flow path length, centroidal flow path dimensions, and sub-basin gradients or slopes.

Model application

The calculations pertaining to the daily stream flow were executed with great precision using the HEC-HMS 4.1 model. This process relied heavily on a meticulously curated compilation of data maps, which served as indispensable inputs. Furthermore, rigorous datasets were employed, encompassing comprehensive records of daily precipitation, river flow statistics, and corresponding evaporation figures. Moreover, the modeling framework necessitated the inclusion of highly detailed input parameters, tailored to accommodate various methods of loss. These parameters included intricate specifications related to variables such as initial deficit, maximum storage capacity, constant rate of precipitation loss, imperviousness, curve number, initial abstraction, initial and saturated contents, suction, and conductivity.

Additionally, the model's operational algorithms required precise input parameters governing unit hydrograph characteristics. These parameters encompassed factors like time of concentration, storage coefficient, lag time, and peaking coefficient. The meticulous selection of these parameters took into account the specific soil type characteristics predominant within the catchment area.

Model calibration

The model underwent a calibration process utilizing datasets encompassing daily rainfall, daily river flow, and daily evaporation from the period spanning 2001 to 2010. This calibration entailed the application of three discrete methodologies to ascertain the optimal approach tailored to the unique characteristics of the study catchment.

Table 1: Loss and Transform methods used for Calibration

LOSS METHOD	TRANSFORM METHOD
Deficit and constant Loss	Clark Unit Hydrograph
SCS Curve Number	Snyder Unit Hydrograph
Green and Ampt	SCS Unit Hydrograph

In a sequential manner, each loss method was conjoined with three distinct transform methods as shown in Table 1. Subsequently, the resultant simulated flow outcomes engendered by each of these diverse loss methods underwent meticulous and rigorous statistical analysis to evaluate their efficacy and integrity.

Deficit and Constant Loss Model

The Deficit and Constant Loss Method introduces a quasi-continuous modification to the conventional initial and constant loss model, focusing on managing precipitation losses. Unlike its standard counterpart, this method uniquely incorporates a gradual regeneration of the initial loss following extended rain-free periods. Its application necessitates the specification of three crucial parameters: the initial loss, the constant loss rate, and the recovery rate. The initial loss denotes the amount of water that must be exceeded before runoff initiates, while the constant loss rate accounts for ongoing water loss due to factors such as evaporation and percolation. What distinguishes this model is the inclusion of the recovery rate, which indicates how quickly the initial loss can replenish itself after prolonged periods without rainfall. This approach monitors the moisture deficit by calculating it as the difference between precipitation volume and initial abstraction, subsequently adjusting for recovery volumes during dry spells. Estimating the recovery rate involves various methods, including amalgamating rates of evaporation and percolation or their components.

At the core of the initial and constant loss model lies the concept of a constant maximum potential rate of precipitation loss, denoted as "fc," during a defined interval. Thus, if "Pt" represents the average precipitation depth over an interval from "t" to "t+Δt," then the surplus precipitation amount, termed "pet," for that interval can be expressed as follows:

$$\left.\begin{array}{ll} Pe_t = Pt - fc & If\ Pt > fc \\ Pe_t = 0 & Otherwise \end{array}\right\} \quad (1)$$

Incorporated within the model is an inaugural loss component denoted as "Ia," serving to encompass interception and depression storage. Interception storage signifies the absorption of precipitation by surface cover elements, encompassing watershed vegetation. Conversely, depression storage results from topographical low points within the watershed; these indentations temporarily retain water, subsequently infiltrating the soil or undergoing evaporation. Notably, this loss transpires antecedent to any runoff commencement. It merits emphasis that runoff only initiates upon cumulative precipitation surpassing the initial loss volume over the previous area. Hence, the remaining surplus runoff is delineated by the ensuing expression:

$$\left.\begin{array}{ll} Pe_t = 0 & If \sum Pi < Ia \\ Pe_t = Pt - fc & If \sum Pi > Ia \ \ and \ \ Pi > fc \\ Pe_t = 0 & If \sum Pi > Ia \ \ and \ \ Pi < fc \end{array}\right\} \quad (2)$$

SCS Curve Number Loss Model

The Soil Conservation Service (SCS) Curve Number model utilizes a mathematical formulation to evaluate the excess precipitation attributable to variables including cumulative precipitation, soil cover, land usage, and antecedent moisture conditions (Lian et.al., 2020). This assessment aims to ascertain the volume of runoff, delineated by the following equation:

$$Pe = \frac{(P-Ia)^2}{P-Ia+S} \quad (3)$$

In the aforementioned equation, Pe symbolizes the cumulative precipitation excess at a specified temporal instance 't,' where P signifies the accumulated depth of rainfall at that identical moment. Furthermore, Ia denotes the initial abstraction, serving as an initial loss factor, while S characterizes the potential maximum retention capacity of a watershed. This parameter S epitomizes the watershed's intrinsic ability to capture and retain storm-induced precipitation.

It warrants emphasis that until the cumulative rainfall surpasses the initial abstraction threshold (Ia), no precipitation excess shall ensue, thereby precluding any runoff generation. Notably, the Soil Conservation Service (SCS), drawing upon extensive scrutiny of diverse empirical data derived from various small-scale experimental watersheds, has delineated a relational model between the initial abstraction (Ia) and the potential maximum retention capacity (S).

$$Ia = 0.2\,S \quad (4)$$

Therefore, the cumulative excess at time t is:

$$Pe = \frac{(P-0.2\,S)^2}{P+0.8\,S} \quad (5)$$

The calculation of incremental surplus within a specified temporal interval necessitates deducting the accumulated surplus at the termination point from that at the inception of said duration. The association between the utmost storage capability (S) of a hydrological basin and its intrinsic attributes is governed by a parameter termed the "curve number," commonly symbolized as CN.

$$S = \frac{1000-10\,CN}{CN} \quad (6)$$

Green and Ampt Loss Model

The Green and Ampt infiltration equation (Mein and Larson, 1973), stands as a prevalent mathematical construct employed for assessing the pace at which water infiltrates into the soil amidst a precipitation occurrence. This model rigorously factors in soil characteristics, initial soil moisture states, and the intensity of rainfall. The equation precisely computes the depletion of precipitation over a pervious region within a specified temporal span.

$$f_t = K\left[\frac{1+(\emptyset-\theta i)S_f}{F_t}\right] \quad (7)$$

The loss over a designated temporal interval, denoted as f(t), is contingent upon variables including the saturated hydraulic conductivity (K), the volumetric moisture deficit (ø – θi), the wetting front suction (Sf), and the cumulative loss up to time t, denoted as Ft. The surplus precipitation on the permeable surface can be computed as the disparity between the Mean Annual Precipitation (MAP) within that period and the loss calculated utilizing Equation (7).

Transform Method

The Unit Hydrograph method is predicated upon the concept of unit hydrographs, which delineate the watershed's response to a standardized precipitation volume during a defined interval. This approach involves the mathematical operation known as convolution, whereby a unit hydrograph is convolved with the actual rainfall distribution, termed a hyetograph, across temporal extents (Roy and Thomas, 2016). This procedure culminates in the derivation of the direct runoff hydrograph tailored to the precise storm occurrence.

Clark Unit Hydrograph

The transient storage of water within a watershed, encompassing reservoirs like soil, surface water, and channels, is crucial for converting surplus precipitation into runoff (Cho et al., 2018). One widely employed approach to capture these complex dynamics is

the linear reservoir model. This model's foundational framework is rooted in the principles of the continuity equation.

$$\frac{ds}{dt} = I_t - O_t \tag{8}$$

Within this context, where dS/dt represents the temporal alteration in water storage at a given moment t, 'I_t' signifies the mean input into storage during that time, and 'O_t' denotes the efflux or discharge from storage at that specific time't.'

In the linear reservoir model, the storage level at time't,' is interconnected with the outflow in the following manner:

$$S_t = R\ O_t \tag{9}$$

By incorporating the constant linear reservoir parameter 'R' into the equations and employing a basic finite difference approach, the equations can be merged and solved to obtain a solution

$$O_t = C_A\ I_t + C_B\ O_{t-1} \tag{10}$$

Where CA, CB = routing coefficients. The coefficients are calculated from:

$$C_A = \frac{\Delta t}{R + 0.5\Delta t} \tag{11}$$

$$C_B = 1 - C_A \tag{12}$$

The average outflow during period t is:

$$\overline{O_t} = \frac{O_{t-1} + O_t}{2} \tag{13}$$

Snyder Unit Hydrograph

Snyder pioneered methodologies aimed at deducing Unit Hydrograph (UH) parameters by correlating them with watershed attributes. His scholarly inquiry pinpointed three pivotal characteristics indispensable for UH scrutiny: lag duration, peak discharge, and the entire temporal span. He formalized a prototype UH where the rainfall duration "tr" interrelates with the basin lag "tp" via the ensuing equation:

$$t_p = 5.5\ t_r \tag{14}$$

Accordingly, given a specific rainfall duration, one can ascertain the lag time (and consequently, the moment when the Unit Hydrograph achieves its maximum) for Snyder's standard Unit Hydrograph. Yet, if the desired Unit Hydrograph duration varies markedly from that defined by Equation 14, one can utilize the subsequent relationship to establish the correlation between the peak time of the Unit Hydrograph and its duration:

$$t_{PR} = t_P - \frac{t_r - t_R}{4} \tag{15}$$

in which tR = duration of desired UH; and tPR = lag of desired UH.

In the standard scenario, Snyder found that the lag and peak of the Unit Hydrograph per unit of excess precipitation per unit area in the watershed exhibited a specific relationship, which can be expressed as:

$$\frac{U_P}{A} = C\frac{C_P}{t_P} \tag{16}$$

Where Up = peak of standard UH; A = watershed drainage area; Cp = UH peaking coefficient; and C = conversion constant (2.75 for SI or 640 for FPS).

For other durations, the UH peak, U_{PR}, is defined as:

$$\frac{U_{PR}}{A} = C\frac{C_P}{t_{PR}} \tag{17}$$

SCS Unit Hydrograph

The essence of the SCS Unit Hydrograph (UH) model lies in a nondimensional UH characterized by a singular crest. This nondimensional UH delineates the discharge, Ut, relative to the peak discharge, Up, of the UH at any moment, quantified as a fraction of Tp, the duration required to attain the UH peak. Studies by the SCS reveal an inherent association between the UH's peak discharge and the duration to attain said peak, expounded as:

$$U_P = C\ \frac{A}{T_P} \tag{18}$$

In the given equation, where A denotes the watershed area and C signifies the conversion constant (2.08 in SI units and 484 in the foot-pound system), the temporal occurrence of the UH peak, colloquially termed the time of rise, is intricately linked to the duration of the unit of excess precipitation as follows:

$$T_P = \frac{\Delta t}{2} + t_{lag} \tag{19}$$

In the given equation, Δt denotes the temporal extent of surplus precipitation (likewise serving as the computational increment throughout the simulation), while tlag denotes the hydrological basin lag, defined as the temporal disparity between the precipitation excess's centroid and the peak of the unit hydrograph.

Statistical evaluation

Nash-Sutcliffe efficiency

The Nash-Sutcliffe Efficiency (NSE) is employed for evaluating the concordance between prognostications of a model and actual data observations. It quantifies the appropriateness of fit by assessing the resemblance in patterns and variability inherent in the observed data. The calculation of NSE involves comparing the squared deviations of predicted values from observed values against the squared deviations of observed values

from their mean. This metric provides insight into the model's fidelity in replicating the observed data dynamics.

$$NSE\ (\eta) = 1 - \frac{\sum_1^n (q_i - Q_i)^2}{\sum_1^n (Q_i - Q)^2}$$

Where,

Qi= Measured stream flow

qi = Simulated stream flow

Q = Average Measured stream flow

n = Total number of time steps in calibration period.

The numerical index known as the Nash-Sutcliffe Efficiency (NSE) serves as a pivotal metric within hydrological simulations, operating within a bounded range from -1 to +1. A positive NSE signifies a superior alignment between simulated data and observed measurements, surpassing the mere mean of observed values. Conversely, a negative NSE denotes substantial divergence between model output and real-world behavior. Notably, an NSE approaching unity indicates a notably robust match between predicted hydrographs and empirical observations, thereby substantiating the model's efficacy. Models yielding negative NSE values are inherently deemed inadequate for the task at hand.

Root Mean Square Error (RMSE)

Root Mean Square Error (RMSE) represents a pivotal statistical measure utilized extensively for assessing the fidelity and precision of predictive models, as well as quantifying discrepancies in observational or predictive data.

Root mean square error (RMSE):

$$RMSE\ = \sqrt{\frac{1}{n}\sum_{i=1}^{n}(q_i - Q_i)^2}$$

R-squared (R^2)

In river flow analysis, R-squared (R^2) assumes a critical role in assessing the extent to which a regression model elucidates the variance observed in river flow data. It quantifies the goodness of fit by gauging the proportion of variability in the dependent variable (river flow) that is explicable by the independent variables (model predictions).

$$R^2 = 1 - \frac{SSE}{SST}$$

In the given formula:

SSE (Sum of Squared Errors) denotes the sum of squared deviations between the observed river flow values and the corresponding predicted values generated by the model.

SST (Total Sum of Squares) quantifies the overall variability observed in the river flow data relative to their mean value.

RESULTS AND DISCUSSION

Runoff by Deficit and Constant Loss Method

The deficit constant loss paradigm necessitates the provision of specific input parameters: the initial deficit quantified in millimeters (mm), the maximal storage capacity also delineated in millimeters (mm), the unvarying rate of loss measured in millimeters per hour (mm/hr), and the extent of imperviousness expressed as a percentage (%). Contrariwise, the Clark unit hydrograph methodology is predicated upon disparate input parameters, specifically the temporal concentration (hours) and the storage coefficient (hours).

The initial computational model was executed utilizing pre-established parameters, with an evaluation of the Nash-Sutcliffe Efficiency (NSE) ensuing. To ascertain the optimal parameter values conducive to achieving a model performance characterized by an NSE surpassing 0.75, strategic modifications were effected on select critical factors. Optimum values of parameters for the three loss methods are shown in Table 2, Table 6 and Table 8 Respectively. These modifications entailed the adjustment of initial loss and constant rate parameters within the deficit constant loss framework, alongside the recalibration of the storage coefficient and temporal concentration parameters inherent in the Clark unit hydrograph transformation method. Additionally, alterations were made to the lag time and peaking coefficient within the Snyder unit hydrograph transformation method. These adjustments were implemented iteratively, with successive refinements, until the statistical evaluation yielded an NSE value exceeding the threshold of 0.75. The optimized parameter values for the three transform methods are shown in Table 3 and Table 4 respectively.

Table 2: Optimized Parameter values: Deficit and Constant Loss Method

Initial Deficit (MM)	Maximum Storage (MM)	Constant Rate (MM/HR)	Impervious (%)
80	135	6	0

Table 3: Optimized parameter values: Clark Unit Hydrograph and Snyder Unit Hydrograph

Transform Methods				
Clark Unit Hydrograph			Snyder Unit Hydrograph	
Time of Concentration (HR)	Storage Coefficient (HR)	Time Area Method	Lag Time (HR)	Peaking Coefficient (HR)
3.2	2.9	Default	1.27	0.68

Table 4: Transform Parameters: SCS Unit Hydrograph

Sub Basin	Graph Type	Lag Time	Sub Basin	Graph Type	Lag Time
S1	Standard (PRF 484)	1110.889765	S13	Standard (PRF 484)	305.3167619
S2	Standard (PRF 484)	681.8695459	S14	Standard (PRF 484)	827.6078716
S3	Standard (PRF 484)	539.3215852	S15	Standard (PRF 484)	630.4442902
S4	Standard (PRF 484)	781.3491286	S16	Standard (PRF 484)	470.3034821
S5	Standard (PRF 484)	538.2297466	S17	Standard (PRF 484)	458.745228
S6	Standard (PRF 484)	1138.464884	S18	Standard (PRF 484)	299.8501847
S7	Standard (PRF 484)	1562.455662	S19	Standard (PRF 484)	891.3628942
S8	Standard (PRF 484)	690.2874485	S20	Standard (PRF 484)	662.7408959
S9	Standard (PRF 484)	658.7067598	S21	Standard (PRF 484)	386.3541802
S10	Standard (PRF 484)	494.989025	S22	Standard (PRF 484)	597.2579341
S11	Standard (PRF 484)	490.2302358	S23	Standard (PRF 484)	537.005948
S12	Standard (PRF 484)	625.1122705			

It is observed that coupling the Deficit and Constant Loss Model with three distinct transform methodologies—namely, the Clark Unit Hydrograph Transform Method, the Snyder Unit Hydrograph Transform Method, and the SCS Unit Hydrograph Transform

Method-produced commendable results in terms of Nash-Sutcliffe Efficiency (NSE), Root Mean Square Error (RMSE), and the coefficient of determination (R^2), as delineated in Table 5. However, the model's predictions for the year 2008 exhibit substantial shortcomings in capturing the inherent variability of the observed data, leading to potential significant deviations from the actual measurements.

Hydrological and environmental models are subject to performance variability across different years due to a myriad of factors, including but not limited to climatic fluctuations and anomalous events. Consequently, while a negative NSE value for a particular year, such as 2008, may signal a deficiency in model accuracy for that period, it does not axiomatically suggest a persistent inaccuracy of the model in general. Such discrepancies underscore the importance of continuous model evaluation and calibration to account for interannual variability and to enhance predictive reliability.

Table 5: Calibration Summary: Deficit and Constant Loss Model

Year	Clark Unit Hydrograph			Snyder Unit Hydrograph			SCS Unit Hydrograph		
	RMSE	R^2	NSE	RMSE	R^2	NSE	RMSE	R^2	NSE
2001	0.3	0.90	0.890	0.3	0.90	0.890	0.3	0.90	0.890
2002	0.5	0.78	0.774	0.5	0.78	0.774	0.5	0.78	0.774
2003	0.4	0.82	0.815	0.4	0.82	0.815	0.4	0.82	0.815
2004	0.5	0.81	0.787	0.5	0.81	0.787	0.5	0.81	0.787
2005	0.3	0.89	0.885	0.3	0.89	0.885	0.3	0.89	0.885
2006	0.3	0.88	0.883	0.3	0.88	0.883	0.3	0.88	0.883
2007	0.5	0.80	0.789	0.5	0.80	0.789	0.5	0.80	0.789
2008	1.1	0.01	-0.113	1.1	0.01	-0.113	1.1	0.01	-0.113
2009	0.3	0.91	0.912	0.3	0.91	0.912	0.3	0.91	0.912
2010	0.4	0.85	0.810	0.4	0.85	0.810	0.4	0.85	0.810

Runoff by SCS Curve Number Loss Method

The parametric refinement of the Soil Conservation Service (SCS) Curve Number loss method was meticulously executed by integrating it with the SCS unit hydrograph technique, thereby attaining Nash-Sutcliffe Efficiency (NSE) indices persistently surpassing the threshold of 0.75, with the singular anomaly being the annum 2003. Utilizing this meticulously optimized parameter ensemble, hydrological runoff simulations were subsequently conducted employing both the Clark unit hydrograph and the Snyder unit hydrograph transformation methods, with each method employing its bespoke optimized parameters as delineated in Table 3.

It was discerned with notable intrigue that, despite the SCS and Clark unit hydrograph methods demonstrating commendable efficacy in model performance metrics, the Snyder unit hydrograph method yielded subpar outcomes when evaluated against critical statistical indicators such as Root Mean Square Error (RMSE), R-squared (R^2), and NSE, as illustrated in Table 7. Notably, there was an absence of negative NSE values across the

simulations, and both the Clark and SCS unit hydrograph methods exhibited satisfactory calibration parameters for the year 2008. This stands in stark contrast to the constant and deficit loss methods, which were markedly less effective in their performance.

Table 6: Parameters: SCS Curve Number Loss Method

Initial Abstraction MM)	Curve Number	Impervious (%)
0	80	0

Table 7: Calibration Summary: SCS Curve Number Loss Model

Year	Clark Unit Hydrograph			Snyder Unit Hydrograph			SCS Unit Hydrograph		
	RMSE	R^2	NSE	RMSE	R^2	NSE	RMSE	R^2	NSE
2001	0.4	0.85	0.826	0.8	0.29	0.282	0.4	0.89	0.853
2002	0.4	0.83	0.817	0.8	0.29	0.284	0.4	0.83	0.807
2003	0.7	0.66	0.577	0.9	0.21	0.147	0.5	0.77	0.736
2004	0.5	0.81	0.753	0.7	0.55	0.532	0.5	0.83	0.792
2005	0.5	0.80	0.779	0.8	0.40	0.389	0.4	0.84	0.803
2006	0.4	0.82	0.810	0.9	0.26	0.257	0.4	0.84	0.828
2007	0.5	0.79	0.768	0.9	0.25	0.233	0.4	0.82	0.811
2008	0.5	0.73	0.704	0.7	0.47	0.457	0.5	0.78	0.770
2009	0.4	0.86	0.845	0.6	0.71	0.657	0.4	0.89	0.863
2010	0.5	0.73	0.730	0.8	0.44	0.432	0.5	0.79	0.785

Runoff by Green and Ampt Loss Method

The Green and Ampt loss method parameters were rigorously optimized, utilizing the calculated values derived from three distinct unit hydrograph transform methodologies (refer to Tables 3 and 4), with the express aim of attaining a Nash-Sutcliffe Efficiency (NSE) coefficient exceeding 0.75. The refined parameters for the Green and Ampt loss method are comprehensively delineated in Table 8, while the outcomes of the calibration process are meticulously encapsulated in Table 9.

Table 8: Loss Parameters: Green and Ampt

Initial Content (MM)	Saturated Content	Suction (MM)	Conductivity (MM/HR)	Impervious (%)
0.1	0.41	142.24	5.08	0.0

Table 9: Calibration Summary: Green and Ampt Loss Model

Year	Clark Unit Hydrograph			Snyder Unit Hydrograph			SCS Unit Hydrograph		
	RMSE	R^2	NSE	RMSE	R^2	NSE	RMSE	R^2	NSE
2001	0.4	0.88	0.877	0.4	0.88	0.877	0.4	0.88	0.877
2002	0.5	0.76	0.750	0.5	0.76	0.750	0.5	0.76	0.750
2003	0.5	0.80	0.791	0.5	0.80	0.791	0.5	0.80	0.791
2004	1.0	0.44	-0.015	1.0	0.44	-0.015	1.0	0.44	-0.015
2005	0.4	0.87	0.874	0.4	0.87	0.874	0.4	0.87	0.874
2006	0.4	0.86	0.860	0.4	0.86	0.860	0.4	0.86	0.860
2007	0.5	0.76	0.749	0.5	0.76	0.749	0.5	0.76	0.749
2008	0.7	0.80	0.490	0.7	0.80	0.490	0.7	0.80	0.490
2009	0.3	0.89	0.885	0.3	0.89	0.885	0.3	0.89	0.885
2010	0.4	0.84	0.808	0.4	0.84	0.808	0.4	0.84	0.808

When the Green and Ampt loss method is synergistically integrated with three distinct transformation methodologies for the calibration years, the resultant metrics—specifically Root Mean Square Error (RMSE), coefficient of determination (R^2), and Nash-Sutcliffe Efficiency (NSE)—exhibit a notable consistency. However, an anomalous manifestation of negative NSE values is observed for the year 2004, indicating a profound deviation from acceptable model performance. Furthermore, the results for the year 2008 are adjudged to be substandard, primarily attributable to NSE values falling below the threshold of acceptability, thereby rendering the model's predictive capability for that year inadequate.

MODEL VALIDATION

Upon meticulous examination of the empirical data encapsulated within Tables 4, 5, and 6, it becomes manifestly evident that the application of the SCS Curve Number (CN) Loss method in conjunction with the SCS unit hydrograph Transform method culminates in the most propitious outcomes for the tropical Wardha river basin. This assertion is substantiated by the superior metrics observed, specifically Root Mean Square Error (RMSE), Coefficient of Determination (R^2), and Nash-Sutcliffe Efficiency (NSE), as delineated in Table 10. Moreover, this synergistic amalgamation of loss and transform methodologies conspicuously eschews any incidence of adverse or unsatisfactory NSE values.

The veracity and pertinence of the model, along with its parameterization, were meticulously verified to ensure their robustness for application across the entire temporal spectrum of observational data within the catchment area. The validation process encompassed an extensive temporal span from 2011 to 2018, leveraging both

meteorological and hydrological datasets. The model parameters, meticulously ascertained through a rigorous calibration process employing diverse methodologies, were meticulously integrated into the model. Subsequent simulation runs during the validation phase affirmed the model's efficacy, with performance metrics during this period mirroring those of the calibration phase (2001-2010), consistently achieving Nash-Sutcliffe Efficiency (NSE) values in excess of 0.75. The simulated and observed stream flow for calibration and validation period by SCS-CN loss model in conjunction SCS unit hydrograph transform method are depicted in Figure 2 and Figure 3 respectively.

Table 10: Validation using SCS Curve Number Loss Model and SCS Unit Hydrograph Transform Model

Year	RMSE	R^2	NSE
2011	0.5	0.78	0.768
2012	0.4	0.81	0.801
2013	0.5	0.79	0.790
2014	0.4	0.84	0.812
2015	0.5	0.80	0.788
2016	0.5	0.79	0.787
2017	0.4	0.84	0.809
2018	0.5	0.80	0.752

The performance evaluation of the Soil Conservation Service (SCS) Curve Number (CN) loss model, in conjunction with the SCS Unit Hydrograph (UH) transform method, during the calibration period unequivocally substantiates the precision of the hydrological data pertaining to the years 2004 and 2008. However, the implementation of the Deficit and Constant (D and C) loss model yielded homogenous results across all three Unit Hydrograph transform methodologies. Conversely, the Snyder Unit Hydrograph exhibited suboptimal performance when employed with the SCS CN loss model.

In the scenario where the Green and Ampt (G and A) loss model was utilized in conjunction with the tripartite Unit Hydrograph transform methods, the results were consistently identical, manifesting in negative or unacceptable Nash-Sutcliffe Efficiency (NSE) values for the hydrological years 2004 and 2008.

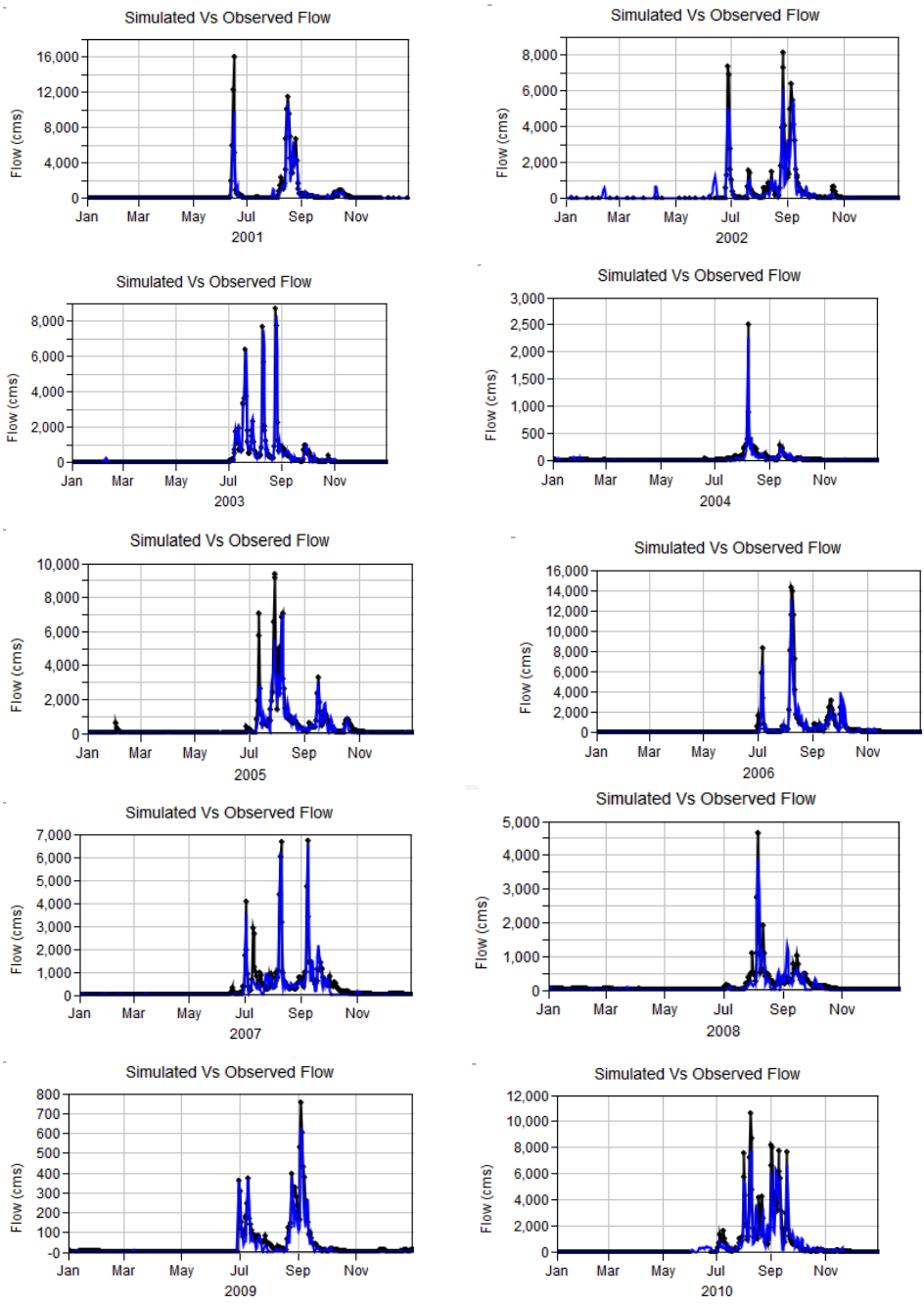

Figure 2: Simulated Vs Observed Flows of Calibration Period (2001-2010)

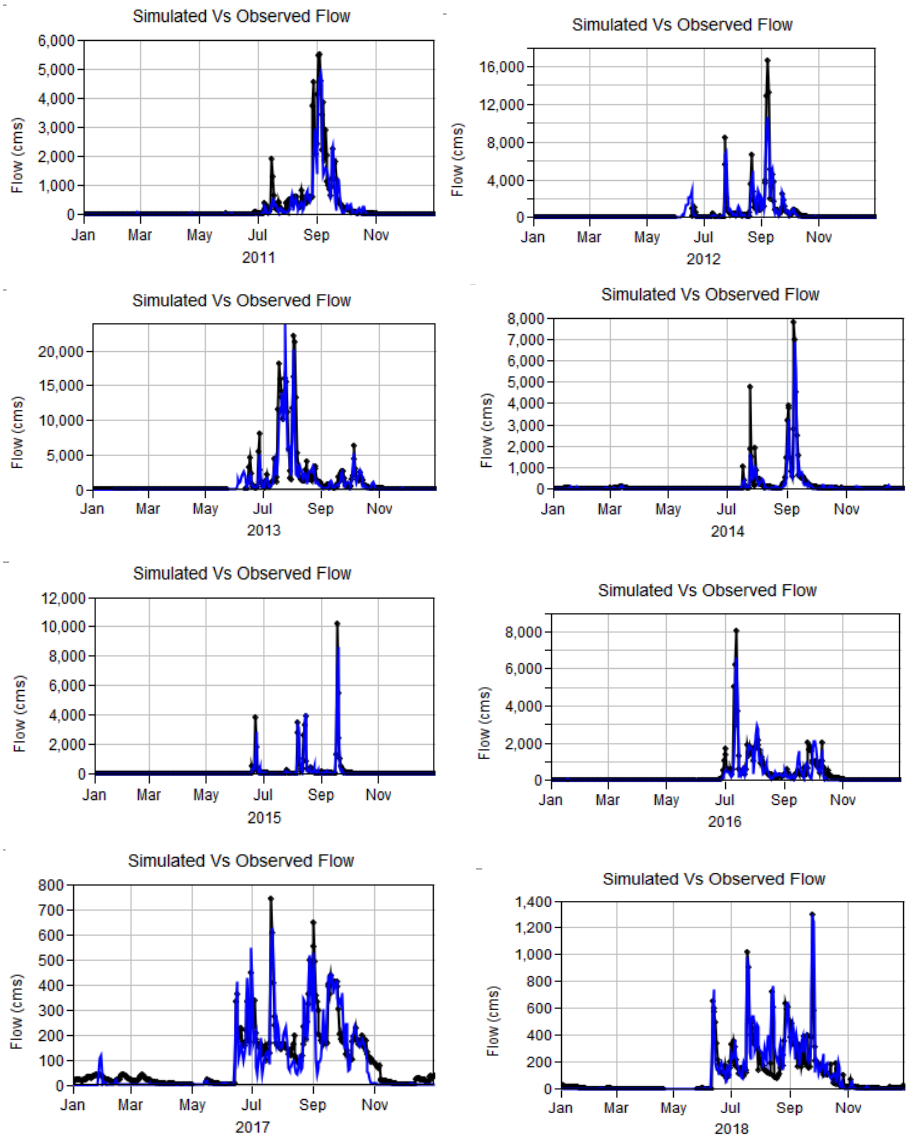

Figure 3: Simulated Vs Observed Flows of Validation Period (2011-2018)

The subpar performance of both the Deficit and Constant loss model and the Green and Ampt loss model during the years 2004 and 2008 can be ascribed to the extended periods of aridity and minimal precipitation observed in those years. These models, inherently designed to perform optimally under typical or average hydrological conditions, encounter significant challenges in accurately simulating hydrological processes during extended drought periods characterized by scant rainfall. This delineates the necessity of

acknowledging the inherent limitations of these models and underscores the exigency of model adjustments or the consideration of alternative models when confronted with extreme or atypical hydrological scenarios. Furthermore, it accentuates the paramount importance of precise and exhaustive data acquisition in the domain of hydrological modelling.

CONCLUSION

The empirical investigations illuminate the preeminent efficacy of an integrated approach in hydrological flow simulations, wherein the Soil Conservation Service Curve Number (SCS-CN) loss methodology, conjoined with the SCS unit hydrograph technique, demonstrated exceptional reliability. This amalgamated paradigm notably surpassed the Clark unit hydrograph and Snyder unit hydrograph methodologies in engendering more precise flow simulations.

It is paramount to emphasize that the employment of the SCS-CN method as the loss mechanism profoundly influenced the performance metrics of the Snyder Unit Hydrograph method, culminating in suboptimal results. Conversely, the Deficit and Constant Loss method, alongside the Green and Ampt loss method, when deployed in conjunction with all three unit hydrograph techniques, produced closely correlated values vis-à-vis an array of statistical parameters, including the Nash-Sutcliffe efficiency coefficient. This uniformity across disparate unit hydrograph methodologies underscores the robustness and reliability of these two loss methods in effectuating hydrological simulations within the specific ambit of the investigation.

Declaration of competing interest

The authors declare that they have no known competing financial interests or personal relationships that could have appeared to influence the work reported in this paper.

REFERENCES

ABD RAHMAN A.N., OTHMAN F., WAN JAAFAR W.J., AHMED ELSHAFIE A.H.K. (2023). An assessment of floods' characteristics and patterns in Pahang, Malaysia, Larhyss Journal, No 55, pp. 89-105.

ATALLAH M., DJELLOULI F., HAZZEB A. (2024). Rainfall-Runoff modeling using the HEC-HMS model for the Mekerra Wadi watershed (N-W Algeria), Larhyss Journal, No 57, pp. 187-208.

BAUDHANWALA D., KANTHARIA V., PATEL D., MEHTA D., WAIKHOM, S. (2023). Applicability of SWMM for urban flood forecasting a case study of the western zone of Surat City, Larhyss Journal, No. 54, pp. 71-83.

BELAY Y. Y., GOUDAY Y. A., ALEMNEW H. N. (2022). Comparison of HEC-HMS hydrologic model for estimation of runoff computation techniques as a design input: case of Middle Awash multi-purpose dam, Ethiopia, *Applied Water Science, Vol. 12, Issue 4, Paper ID 237.*

BEKHIRA A., HABI M., MORSLI B. (2019). The management of flood risk and development of watercourses in urban areas: case of the town of Bechar, Larhyss Journal, No 37, pp. 75-92. (In French)

BENALI KHODJA M., FERDJOUNI N. (2024). Assessment of the meteorological drought in the northern part of Algeria - Case of the Isser wadi watershed, Larhyss Journal, No 58, pp. 39-54.

CHIBANE B., ALI-RAHMANI S.E. (2015). Hydrological based model to estimate groundwater recharge, real- evapotranspiration and runoff in semi-arid area, Larhyss Journal, No 23, pp. 231-242.

CHO Y., ENGEL B. A., MERWADE V. M. (2018). A spatially distributed Clark's unit hydrograph based hybrid hydrologic model (Distributed-Clark), *Hydrological Sciences Journal,* Vol. 63, Issue 10, pp. 1519-1539.

FELDMAN (2000). *Hydrologic Modeling System HEC-HMS: Technical Reference Manual,* US Army Corps of Engineers, Hydrologic Engineering Center.

FERNANDO H.M.S., GUNAWARDENA M.P., NAJIM M.M.M. (2021). Modelling of stream flows of a forested catchment in the tropics using HEC-HMS, Larhyss Journal, No 48, pp. 73-89.

HAFNAOUI M.A., MADI M., BEN SAID M., BENMALEK A. (2022). Floods in El Bayadh city: causes and factors, Larhyss Journal, No 51, pp. 97-113.

HAFNAOUI M.A., BOULTIF M., DABANLI I. (2023). Floods in Algeria: analyzes and statistics, Larhyss Journal, No 56, pp. 351-369.

HALWATURA D., NAJIM M. M. M. (2013). Application of the HEC-HMS model for runoff simulation in a tropical catchment, *Environmental Modelling and Software, Vol. 46,* pp. 155-162.

HAMDAN A. N. A., ALMUKTAR S., SCHOLZ M. (2021). Rainfall-Runoff Modeling Using the HEC-HMS Model for the Al-Adhaim River Catchment, Northern Iraq, *Hydrology, Vol. 8, Issue 2, Paper ID* 58.

HAO Z., SINGH V. P., XIA Y. (2018). Seasonal drought prediction: Advances, challenges, and future prospects, *Reviews of Geophysics, Vol. 56, Issue 1,* pp.108-141.

HERRERA P.A., MARAZUELA M.A., HOFMANN, T. (2022). Parameter estimation and uncertainty analysis in hydrological modelling, Wiley Interdisciplinary Reviews: Water, Vol. 9, Issue 1, pp. 1-23.

KAMAGATE B., DAO A., NOUFE D., YAO K.L., FADIKA V., GONE D.L., SAVANE I. (2017). Contribution of Gr4j model for modeling Agneby watershed runoff in southeast of Cote d'Ivoire, Larhyss Journal, No 29, pp. 187-208. (In French)

KAPADIA C., PATEL, K., AKBARI J., RATHOD N., MEHTA D., WAIKHOM S. (2023). Flood hazard mapping of lower Damanganga river basin using multi-criteria analysis and geoinformatics approach, Larhyss Journal, No 55, pp. 73-87.

KHERDE R.V., SAWANT P.H. (2018). Parameter Optimization, Uncertainty Estimation and Sensitivity Analysis in Hydrological Modeling, *European Journal of Engineering and Technology Research, Vol. 3, Issue 11,* pp. 66–72.

KOUA T., ANOH K., EBLIN S., KOUASSI K., KOUAMEK., JOURDA J. (2019). Rainfall and runoff study in climate change context in the Buyo lake watershed (southwest Côte d'Ivoire), Larhyss Journal, No 39, pp. 229-258. (In French)

KOUAMÉ K.A., KOUDOU A., SOROKOBY V.M., KOUAMÉK. F., KOUASSI A.M. (2017). Relationship between surface and underground water flow in the upper Bandama watershed in Ivory Coast, Larhyss Journal, No 29, pp. 137-152. (In French)

KUPZIG J., REINECKE R., PIANOSI F., FLÖRKE M., WAGENER T. (2023). Towards parameter estimation in global hydrological models, *Environmental Research Letters, Vol. 18,* Issue 7, pp. 1-10.

LIAN H., YEN H., HUANG J.C., FENG Q., QIN L., BASHIR M. A., WU S., ZHU A.X., LUO J., DI H., LEI Q., LIU H. (2020). CN-China: Revised runoff curve number by using rainfall-runoff events data in China, Water Research, Vol. 177, Paper ID 115767.

LIN Q., LIN B., ZHANG D., WU J. (2022). Web-based prototype system for flood simulation and forecasting based on the HEC-HMS model, *Environmental Modelling and Software, Vol. 158,* Paper ID 105541.

LIU D., GUO S., SHAO Q., LIU P., XIONG L., WANG L., HONG X., XU Y., WANG Z. (2018). Assessing the effects of adaptation measures on optimal water resources allocation under varied water availability conditions, *Journal of Hydrology, Vol. 556,* pp. 759-774.

MEHTA D., DHABUWALA J., YADAV S. M., KUMAR V., AZAMATHULLA H. M. (2023). Improving flood forecasting in Narmada river basin using hierarchical clustering and hydrological modelling, Results in Engineering, Vol. 20, Issue 10, Paper ID 1571.

MEIN R. G., LARSON C. L. (1973). Modeling infiltration during a steady rain, *Water Resources Research, Vol. 9, Issue 2,* pp. 384–394.

NAKOU T.R., SENOU L., ELEGBEDE B., CODO F.P. (2023). Climate variability and its impact on water resources in the lower mono river valley in Benin from 1960 to 2018, Larhyss Journal, No 56, pp. 215-234.

RAFIEI E.A., KAPPAS M., FASSNACHT S. (2018). Uncertainty analysis of hydrological modeling in a tropical area using different algorithms, *Frontiers in Earth Science, Vol. 12,* pp. 661–67.1

RAD S., JUNFENG D., JINGXUAN X., ZITAO L., LINYAN P., WAN Z. (2022). Lijiang flood characteristics and implication of karst storage through Muskingum flood routing via HEC-HMS, S. China, *Hydrology Research, Vol. 53, Issue 12,* pp. 1480–1493.

REMINI B. (2023). Flash floods in Algeria, Larhyss Journal, No 56, pp. 267-307.

ROUISSAT B., SMAIL N. (2022). Contribution of water resource systems analysis for the dynamics of territorial rebalancing, case of Tafna system, Algeria, Larhyss Journal, No 50, pp. 69-94.

ROY A., THOMAS R. (2016). A Comparative Study on the Derivation of Unit Hydrograph for Bharathapuzha River Basin, *Procedia Technology, Vol. 24,* pp. 62-69.

SARDOII E. R., RADMANESH F., SHAMSIPOUR A., ZAREI A. (2012). Calibration of loss estimation methods in HEC-HMS for simulation of surface runoff (Case Study: Amirkabir Dam Watershed, Iran), *Advances in Environmental Biology, Vol. 6, Issue 1,* pp. 343-348.

U.S. ARMY CORPS OF ENGINEERS (2008). *Hydrologic Modeling System (HEC-HMS) Applications Guide: Version 3.1.0,* Institute for Water Resources, Hydrologic Engineering Center, Davis, CA, USA.

VERMA S., VERMA M. K., PRASAD, A. D., MEHTA D., AZAMATHULLA H. M., MUTTIL N., RATHNAYAKE U. (2023). Simulating the hydrological processes under multiple land use/land cover and climate change scenarios in the mahanadi reservoir complex, Chhattisgarh, India, Water, Vol. 15, Issue 17, Paper ID 3068.

VERMA S., VERMA M. K., PRASAD A. D., MEHTA D. J., ISLAM M. N. (2024). Modelling of uncertainty in the estimation of hydrograph components in conjunction with the SUFI-2 optimization algorithm by using multiple objective functions, Modelling Earth Systems and Environment, Vol. 10, Issue 1, pp. 61-79.

YUAN W., LIU M., WAN F. (2019). Calculation of Critical Rainfall for Small-Watershed Flash Floods Based on the HEC-HMS Hydrological Model, *Water Resources Management, Vol. 33,* pp. 2555–2575.